

See discussions, stats, and author profiles for this publication at: <https://www.researchgate.net/publication/230887392>

Low Temperature Studies of Iron-Catalyzed Cross-Coupling of Alkyl Grignard Reagents with Aryl Electrophiles

ARTICLE *in* ADVANCED SYNTHESIS & CATALYSIS · FEBRUARY 2012

Impact Factor: 5.66 · DOI: 10.1002/adsc.201100392

CITATIONS

19

READS

42

5 AUTHORS, INCLUDING:



[Per-Fredrik Larsson](#)

AkzoNobel

9 PUBLICATIONS 221 CITATIONS

SEE PROFILE



[Per-Ola Norrby](#)

University of Gothenburg

181 PUBLICATIONS 5,206 CITATIONS


SEE PROFILE

Low Temperature Studies of Iron-Catalyzed Cross-Coupling of Alkyl Grignard Reagents with Aryl Electrophiles

Jonatan Kleimark,^a Per-Fredrik Larsson,^a Parisa Emamy,^a Anna Hedström,^a and Per-Ola Norrby^{a,*}

^a University of Gothenburg, Department of Chemistry, Kemigården 4, SE-412 96 Göteborg, Sweden
Fax: (+46)-31-772-1394; phone: (+46)-31-786-9034; e-mail: pon@chem.gu.se

Received: May 16, 2011; Revised: September 26, 2011; Published online: January 19, 2012

 Supporting information for this article is available on the WWW under <http://dx.doi.org/10.1002/adsc.201100392>.

Abstract: The title reaction has been studied under low temperature conditions. Coupling with active substrates can be done even at dry ice temperature. Initial rate studies at -25°C indicate that high concentrations of any reagent can lead to either complete or partial catalyst deactivation. Under strongly reducing conditions, iron seems to form less active complexes that only slowly re-enter the catalytic

cycle, possibly through bimolecular coupling of iron(II) complexes. Computational studies support the experimental observations, and indicate that oxidation states below +I cannot be reached by reductive elimination.

Keywords: cross-coupling; density functional calculations; iron; kinetics; reaction mechanism

Introduction

Metal-catalyzed cross-coupling reactions have been some of the most important classes of reactions in organic synthesis for decades. Reactions such as the Suzuki, Heck, Negishi and Ullmann are today widely used tools in synthetic laboratories and constitute essential steps in the synthesis of drugs and other fine chemicals.^[1] The most prominent example of these reactions are the Pd-catalyzed cross-couplings, which can be performed under mild conditions and tolerate many functional groups.^[2] Among the potential drawbacks can be mentioned the high price of noble metals and their ligands, potential leaching of the catalyst to the environment or the product, and in some cases (e.g., the Stille reaction) production of toxic waste. Investigations into alternative catalysts can potentially alleviate these problems while at the same time providing interesting differences in scope and reactivity.

Iron salts have been utilized in cross-coupling reactions since the 1940s,^[3] but the Pd- and Ni-catalyzed versions have come to dominate the area since their introduction in the 1970s,^[4] with only occasional reports on the use of iron.^[5] Since the mid-1990s, the interest in the environmentally friendly iron-catalyzed reactions has increased, and several groups have contributed to broaden the scope and elucidate the mech-

anism.^[6] One important and useful feature of iron catalysis is the ability to catalyze couplings with alkyl substrates without significant β -elimination, a task that can be problematic within the nickel triad of catalysts.^[7] Despite substantial recent progress,^[8] we still need to increase our knowledge of the mechanism of iron-catalyzed couplings, in order to enable a rational selection of reaction conditions and ligands.

In the 1970s, Kochi et al. performed kinetic studies on the iron-catalyzed coupling between Grignard reagents and organic halides.^[5a] The reaction showed first-order dependence in both iron catalyst and alkyl halide, and was virtually independent of the concentration of the Grignard reagent. With support of the by-product profile and EPR measurements,^[9] Kochi proposed an Fe(I) [or possibly Fe(0)] active catalyst and suggested a Kumada–Tamao–Corriu^[4] type catalytic cycle.^[10] This view was later challenged when it was discovered that Fe(–II) complexes act as efficient pre-catalysts in the iron-catalyzed couplings, and the dominating view in the last decade has been that iron cycles between oxidation states –II and 0 in the catalytic cycle.^{[11][12]}

We recently studied the title reaction by a combination of reaction monitoring, competitive Hammett studies, and DFT modelling.^[13] We found strong support for the Fe(I)–Fe(III) cycle, with oxidative addition as rate-limiting step. Interestingly, our computa-

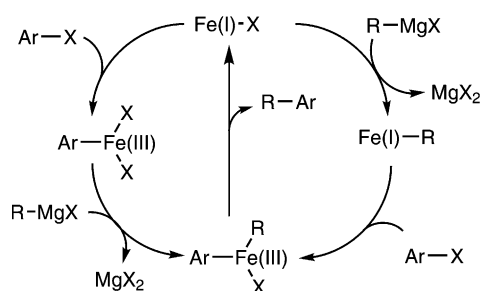


Figure 1. Two feasible catalytic cycles for the coupling reaction.^[13]

tional study indicated the feasibility of two similar cycles, where the transmetalation can precede or follow the oxidative addition (Figure 1).

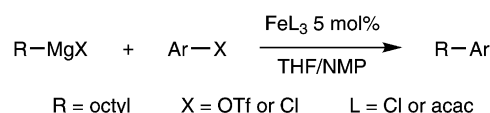
During the course of our further research in this area, we could verify something that already had been proposed in the literature – that the title reaction could be performed at significantly lower temperatures than the standard cross-coupling reaction. Some of the couplings could even be carried out at -78°C , a feature that may be utilized to achieve better regio- or enantioselectivity and higher functional group tolerance. Ability to perform couplings at decreased temperatures is rare in the metal-catalyzed cross-coupling family, with only a few examples reported in the literature.^[6j,7,11a,14] Therefore, we decided to investigate the catalytic behavior at low temperature in more detail.

In the current study we present our examination of the low-temperature iron-catalyzed cross-coupling reaction, noting in particular differences from the behavior at ambient temperature. The scope and reactivity for the reaction at low temperatures is investigated. Furthermore, a kinetic investigation to reveal the influence of all the reacting species in the title reaction is presented. The experiments are supported by computational investigations. The results from the experiments and calculations allow us to reach several new and exciting conclusions concerning the reaction conditions and the mechanism of the reaction. Interestingly, the conditions from the kinetic investigation give us the opportunity to understand, in detail, the different pathways to catalyst deactivation and how to avoid them.

Results and Discussion

Reactivity at Low Temperatures

A selection of different aryl electrophiles was screened for their ability to couple with an alkyl Grignard reagent at three different temperatures: -78°C , -20°C , and ambient temperature (Scheme 1). For all reactions, we followed the previously estab-



Scheme 1. The title reaction, iron-catalyzed cross-coupling between alkyl Grignard reagent and aryl electrophile.

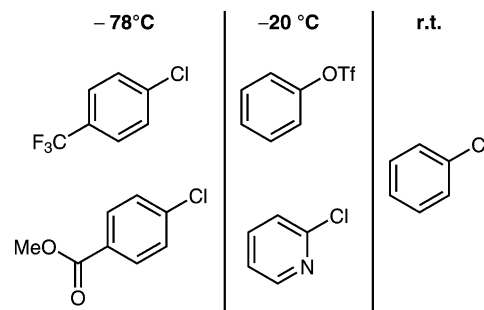


Figure 2. Competent substrates at different temperatures.

lished protocol of adding the Grignard reagent in small portions at intervals (*ca.* 15 min), to avoid the precipitation of catalyst that had been observed at high concentrations of Grignard reagent.^[13] Reactions were monitored by GC, and judged successful if a significant amount ($> 50\%$) of product could be detected after complete addition.

The tested substrates are depicted in Figure 2. As can be seen, only aryl chlorides with a strongly electron-withdrawing group were competent coupling partners at -78°C . Other substrates showed no conversion at this low temperature. Chloropyridine was successfully coupled at -20°C . At this temperature, unsubstituted chlorobenzene was still unreactive, but phenyl triflate reacted well, showing that triflate is a better leaving group than chloride in these reactions. Unactivated chlorobenzene required ambient temperature for significant coupling activity. These results are well in line with the earlier reported, strongly positive ρ -value in a room temperature Hammett study,^[13] and also agree well with the hypothesis of a rate-limiting oxidative addition.

Computational Study of the Oxidative Addition

A computational investigation was performed in order to give an explanation to the results from the substrate screen. Since the rate-limiting step for this reaction is the oxidative addition, we therefore calculated barriers for oxidative addition of Fe(I) to selected substrates (Table 1). We can see that the calculated barriers agree reasonably well with the experimental results in Figure 2. The highest barrier is found for the only substrate requiring room temperature, chlorobenzene. Phenyl triflate has a lower barrier,

Table 1. Calculated barriers to oxidative addition for selected substrates.

Substrate	ΔE^\ddagger (kJ mol ⁻¹)
phenyl-Cl	65
phenyl-OTf	52
<i>p</i> -CF ₃ -phenyl-Cl	49
2-Cl-pyridine	40

and that for CF₃-substituted chlorobenzene is even lower, as expected. Somewhat surprisingly, the lowest barrier overall was found for 2-chloropyridine, a substrate that was only active at -20°C . We speculate that the moderate observed reactivity of this substrate could be due to complexation of the nitrogen lone pair, to magnesium or iron, in a geometry that retards the oxidative addition. We also note that this was the only substrate that would give coupling product without iron catalyst at room temperature, presumably through an S_NAr reaction.

Low Temperature Kinetic Study

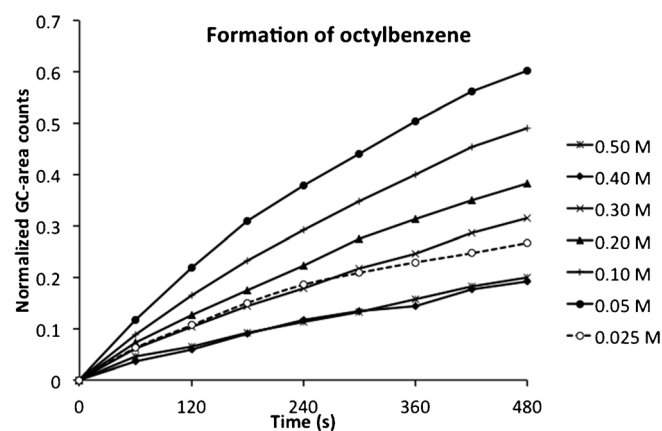
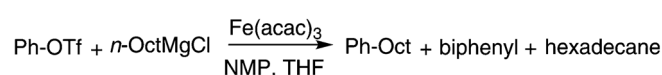
The kinetic investigation was designed as an initial-rate study at -25°C , of the reaction between octyl-magnesium chloride and phenyl triflate, with Fe(acac)₃ as catalyst (Scheme 1). The standard reaction employed 0.5 mmol each of substrate and Grignard reagent, with 0.025 mmol (5 mol%) of iron catalyst. The total reaction volume was adjusted to 20 mL in all cases. The initial concentration of each reagent was varied systematically. Reaction progress was followed by GC monitoring of product formation up to *ca.* 10% conversion. This method ensures that plots should be linear unless changes in the reaction mechanism occur in the course of the experiment. Non-linearity in the plots under conditions where all concentrations are approximately constant must be interpreted as a significant change in the catalytic species.

From the previously suggested mechanism with a rate-limiting oxidative addition (Figure 1), we would expect the reaction to be first order in substrate and catalyst, whereas the reaction order in Grignard reagent could vary between 0 and 1 depending on whether transmetalation occurs before or after the oxidative addition step. Our earlier study left this question unresolved;^[13] indeed, both paths could well be followed in parallel.

The active Fe(I) catalyst is formed from the Fe(III) precursor by two transmetalations followed by reductive elimination. Consistent with this, hexadecane was detected in all reaction mixtures, roughly proportional to the amount of iron used in each reaction.

Grignard Reagent

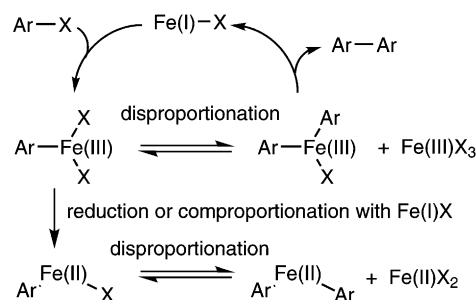
Starting from the lowest concentration of Grignard reagent, 0.025 M, the reaction rate increases when the concentration is doubled (Figure 3), indicating participation of the Grignard reagent in the rate-limiting step. The curvatures of both plots show that the catalyst is slowly deteriorating. At higher concentrations of Grignard reagent, the catalytic performance is decreasing, reaching a minimum at 0.4 M and then staying constant when the loading is increased to 0.5 M. After the first minute at these two highest concentrations, the reaction rate seems to be constant, and independent of the concentration of Grignard. Comparative F-tests for the series at 0.5 M shows that the most significant line is obtained by dropping the first point only, starting the analysis 60 s into the experiment. From this point, the data is a straight line with $r^2 > 0.998$, showing that the rate is constant, independent of Grignard reagent, and that the catalyst is not further deactivated after the first minute. The behavior at 0.4 M is virtually identical, whereas the catalyst deactivation is less significant at the lower concentrations of Grignard reagent (the plots at 0.3 M and below show curvature throughout). Overall, the behavior is consistent with a dual catalyst activity, where the initially formed, highly active catalyst is converted by excess Grignard reagent into a less active form. The higher the Grignard concentration, the faster the catalyst deteriorates to the less active form. Taking into account the strongly reducing power of Grignard reagents, we can speculate that iron in lower oxidation states gives less efficient catalytic cycles. We will return to this point later, in connection with our computational studies (*vide infra*). We also note minor formation of biphenyl at the two lowest Grignard

**Figure 3.** GC monitoring of product formation at different Grignard concentrations.

concentrations, but this is suppressed to insignificant levels at higher concentrations.

Phenyl Triflate

The initial concentration of phenyl triflate was varied in the range 0.025–0.2 M. The reaction order was positive, with a clear increase in initial rate with increasing concentration (Figure 4). Catalyst deactivation occurred in all runs, but especially at the highest concentration of phenyl triflate, where the catalyst died suddenly after 4 min. This is somewhat surprising, as earlier reports suggest that high substrate concentration can protect the integrity of the catalyst.^[13] However, the experimental set-ups differ substantially. In the previous study, the Grignard reagent was added in small aliquots, ensuring that there was never a large excess of Grignard reagent with respect to the catalyst. In the current study, there is sufficient Grignard reagent present to provide a constantly reducing environment. Still, we did not expect that the catalyst



Scheme 2. Plausible disproportionation paths to multiply arylated iron species.

should deactivate more rapidly upon increasing the concentration of the “oxidant”, phenyl triflate. To rationalize this behavior, we must postulate that there are several mechanisms for deactivating the catalyst. In addition to the already proposed deactivation mode based on reduction of Fe, yielding a less efficient but still active catalyst (*vide supra*), there must also be a deactivation mode based on reaction with the arylating reagent.

It has been noted earlier that poly-aryl iron species are stable enough to isolate,^[15] and thus would not be expected to be effective catalysts. Addition of multiple aryl groups to the same iron center could occur in exchange reactions between iron centers (Scheme 2), or by a series of oxidative addition and electron transfer reduction steps. If this is occurring, higher concentrations of phenyl triflate should result in significant production of biphenyl by reductive elimination from diphenyl Fe(III) complexes in solution. This is indeed observed; biphenyl production seems to increase more rapidly than the desired product, octylbenzene, upon increasing the phenyl triflate concentration, see Figure 5. Biphenyl production is also terminated abruptly after 3 min at the highest concentration of phenyl triflate, indicating complete conversion of all iron into a catalytically incompetent polyaryl complex. We can only speculate what this could be. It is plausible that a symmetric $\text{Ph}_4\text{Fe(III)}$ anion^[6e,15] would be reluctant to undergo reductive elimination. However, under the strongly reducing conditions of the current study, another reasonable candidate for the inactive state of iron is a neutral $\text{Ph}_2\text{Fe(II)}$ complex (Scheme 2), since we know that Fe(II) has a high barrier to reductive elimination.^[13]

Iron Catalyst

The catalyst loading was varied from 0.25–5 mM, corresponding to 1–20 mol%. As with the other reagents, at low concentrations the reaction order was positive, with increasing initial rates up to *ca.* 2 mM (Figure 5). With the most dilute catalyst, the reaction was close

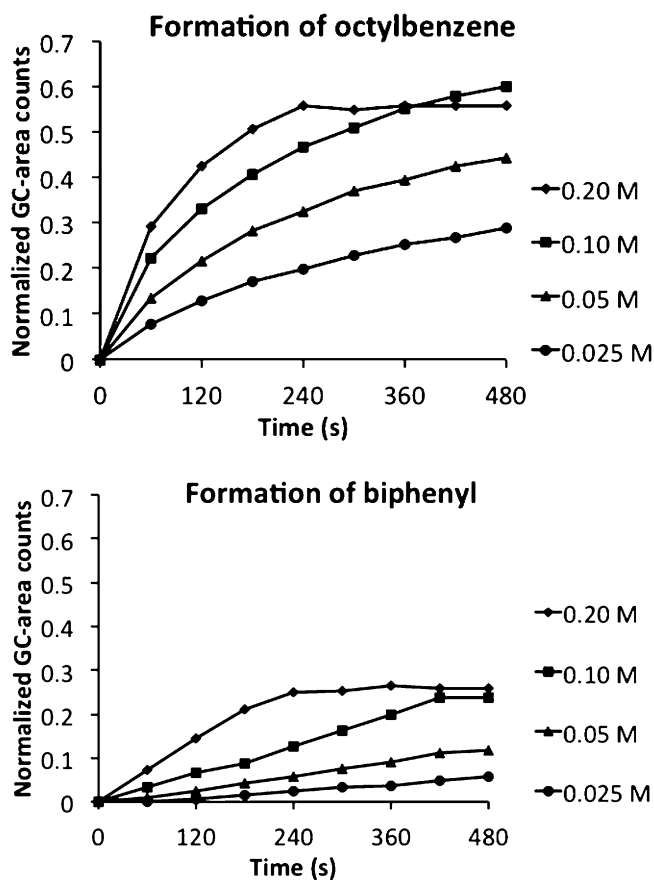
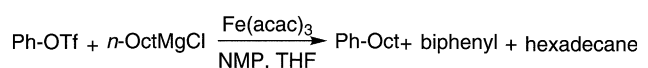


Figure 4. Formation of octylbenzene and biphenyl at varying concentrations of phenyl triflate.

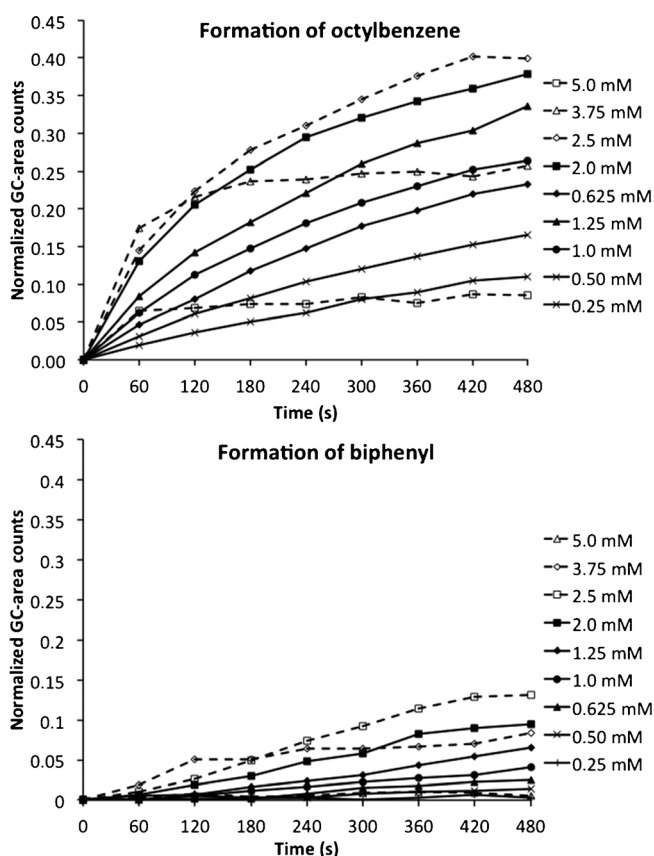
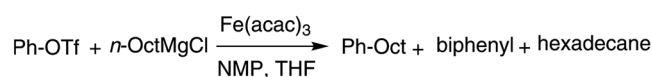


Figure 5. Formation of octylbenzene and biphenyl at varying concentrations of iron catalyst.

to linear, indicating that in this particular reaction, catalyst deterioration was largely suppressed. At higher concentrations, the curvature became more noticeable, and at the highest catalyst concentrations,

sudden catalyst death was observed, similar to what was seen in the phenyl triflate series. This is a strong indication that catalyst deactivation is bimolecular in nature. It has been shown that reductive elimination from mono-nuclear Fe(II) is disfavored, but also that a binuclear mechanism involving two Fe(II) is facile, albeit with a higher barrier than is observed for the proposed Fe(I)-Fe(III) cycle.^[13] The current results can be rationalized if Fe(I) and Fe(III) species in the reaction mixture disproportionate to Fe(II) complexes that react to products in a slow, bimolecular step, reforming Fe(I). Catalyst death could then be rationalized by formation of stable, unreactive Ph_nFe complexes through similar processes. As in the case of high phenyl triflate concentration, increased levels of biphenyl at higher iron concentration gives support for the hypothesis that multiply phenylated iron species are formed in solution.

Computational Study of the Hypothetical Fe(0)-Fe(II) Catalytic Cycle

The results from the kinetic investigation suggest that under strongly reducing conditions, the reaction can drop out of the highly active Fe(I)-Fe(III) cycle, entering a cycle with lower activity. For comparison, we have here calculated barriers for a hypothetical Fe(0)-Fe(II) cycle, to investigate whether such a mechanism could be responsible for the lower activity observed at high Grignard concentrations. For details of the calculations, such as the number of explicit solvent molecules tested, see the Computational Details section.

Somewhat surprisingly, the results depicted in Figure 6 indicate that all steps in the Fe(0)-Fe(II) cycle are less efficient than those in the Fe(I)-Fe(III) cycle. Common wisdom would indicate that if a free

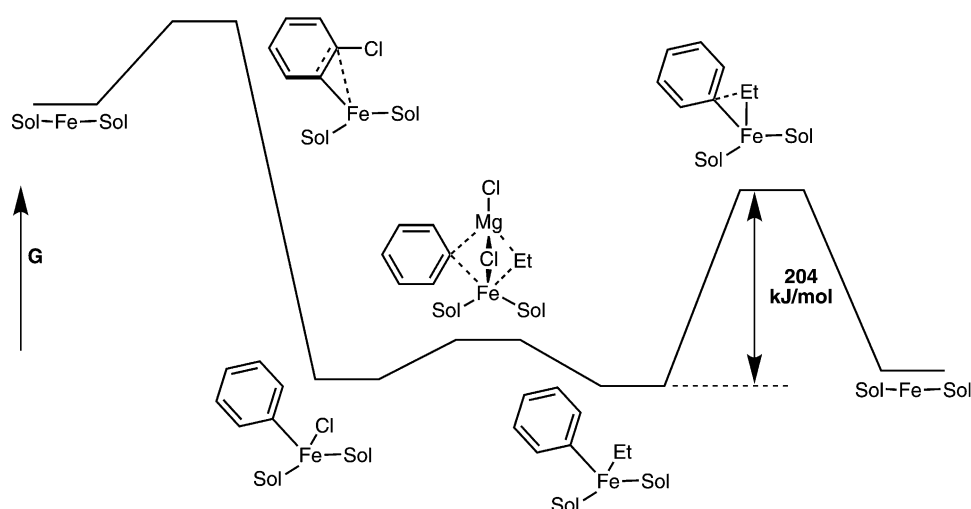


Figure 6. Free energy surface for the hypothetical Fe(0)-Fe(II) cycle.

Fe(0) species existed in solution, it would be more efficient in oxidative addition than the Fe(I) species. However, this is not observed, possibly because the oxidative addition is more complex than a pure redox reaction, also involving coordination of the aromatic π -system to Fe. The barrier is a rather modest 87 kJ mol^{-1} , higher than for Fe(I), but not incompatible with a catalytic cycle even at low temperature. As before, transmetalation has an insignificant barrier, occurring easily in a bimetallic complex. The plateau for the bimetallic complex shown in Figure 6 is in fact not a transition state, but an energy minimum. At the potential energy surface, this is lower in energy than the separated species flanking it. The separations, either forward or backward, are monotonic processes on the PES, occurring without saddle points, indicating very low free energy barriers.^[16] However, the reductive elimination is prohibitive at 204 kJ mol^{-1} , making it completely impossible to reform Fe(0) by reductive elimination from the Fe(II) complex shown in Figure 6. Ligands like alkenes (present in the reaction mixture as impurities in the Grignard reagent) could potentially lower this barrier by stabilizing the Fe(0) state. To investigate this possibility, we performed a computational study where one or both of the solvent molecules in Figure 6 were replaced by the simple model alkene ethene (see Computational Details section and the Supporting Information for further details). Replacement of one solvent with ethene in the Fe(II) complex resulted in a modest stabilization by *ca.* 6 kJ mol^{-1} , further replacement resulted in an equally large destabilization, with the diethene complex showing similar stability as the original solvent complex. The transition states for the subsequent reductive elimination were identified and the barriers were found to be 144 and 129 kJ mol^{-1} , for the solvato-ethene and diethene complexes, respectively, giving Fe(0)-alkene complexes. Thus, in the presence of substantial amounts of alkene, these paths become feasible at higher temperatures, but improbable at the low temperatures examined here. Comparing to the barrier calculated earlier for reductive elimination from a bis-Fe(II) complex giving two Fe(I) complexes, 85 kJ mol^{-1} ,^[13] we can conclude that the reaction giving Fe(I) should be strongly favored over pathways leading to Fe(0).

It should be noted that heterogeneous Fe(0) can be formed from the reaction of Grignard reagents with simple iron salts.^[17] However, the current results indicate that in the presence of substrates like phenyl triflate, oxidative addition will outcompete Fe(0) formation.

Mechanism under Reducing Conditions

From the combined results from the kinetic investigation and the computational study, we can draw several interesting conclusions. Our previous study has shown that under slow addition conditions, so that the concentration of Grignard reagent does not exceed iron concentration, the reaction follows a simple Fe(III)-Fe(I) cycle.^[13] The current results clearly indicate that in the presence of high concentrations of Grignard, the catalyst becomes less active (Figure 3). This lower activity cannot be simple Grignard addition to either Fe(III) or Fe(I), since these processes are part of the fast catalytic cycle depicted in Figure 1. The most probable remaining option is that the most easily susceptible complex in the catalytic cycle, ArFe(III)X_2 , is reduced, either by single electron transfer (SET) from excess Grignard reagent or, as depicted in Figure 7, by comproportionation with Fe(I) species. This would lead to Fe(II) complexes that could easily undergo transmetalation, but would be unable to undergo direct reductive elimination at these low temperatures (*vide supra*) and would only slowly return to the “normal” catalytic cycle through a bimetallic coupling process.^[13]

The side path depicted in Figure 7 is hypothetical, but it does explain the reduced reactivity at high concentrations of iron and/or Grignard, since increased Grignard concentration will result in a higher proportion of iron in lower oxidation state (here +I). Other reaction mechanisms could also explain the observed retardation, but the constraints imposed by our computational studies seem to exclude iron oxidation states below +I. Thus, the intermediacy of Fe(II) complexes in a slower side cycle seems the most plausible candidate for explaining the activity lowering when the Grignard concentration is increased.

We note that the mechanism in Figure 7 does not explain the sudden catalyst death observed at high

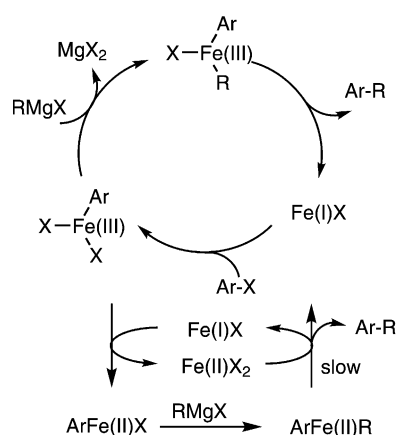


Figure 7. Plausible catalytic cycles under reducing conditions.

concentrations of PhOTf. However, transmetallation among iron complexes could presumably produce inactive Ar_2Fe or more highly arylated species.^[6e,15]

Conclusions

The title reaction shows extreme reactivity in C–C couplings, with facile reactions even at dry ice temperatures. However, the scope at this low temperature is limited. Only aryl chlorides with strongly electron-withdrawing groups are competent substrates. The reaction scope was wider at -20°C , but still required electron deficient substrates, or the triflate leaving group. The low temperature protocol allows C–C coupling with Grignard reagents even in the presence of moderately sensitive functional groups like esters.

Kinetic investigations at -25°C were in agreement with the previously proposed Fe(I)-Fe(III) catalytic cycle when all reactants were diluted. Potentially problematic catalyst deactivations pathways were identified. Most importantly, excess Grignard reagent produced reduced iron complexes with low activity, explaining the observed benefit of slow addition protocols. Completely inactive complexes were produced when the concentration of either iron or phenyl triflate was high.

Computational investigations have shown good agreement between observed reactivity of different substrates and calculated barriers for oxidative addition to Fe(I). It could also be shown that formation of Fe(0) has a prohibitively high barrier, but that Fe(II) complexes can re-enter the catalytic cycle in a slow, binuclear step. The resulting Fe(I)-Fe(III)-Fe(II) cycle is currently the most plausible proposal for the slower reaction observed at the later stages of the monitoring in the reducing environment when high concentrations of Grignard reagents are employed.

Experimental Section

Computational Details

As model for the Grignard reagent we use ethylmagnesium chloride ($\text{C}_2\text{H}_5\text{MgCl}$). The THF solvent is modelled by a variable number of directly coordinated dimethyl ether molecules (CH_3OCH_3). All possible spin configurations have been considered. The actual number of explicit solvent molecules for each complex is determined by the final free energy (*vide infra*). With this explicit solvation, geometries are determined in vacuum using the Jaguar program^[18] but final energies are determined in conjunction with a continuum solvation model with parameters suitable for THF.^[19] All calculations employ the B3LYP functional^[20] in conjunction with the LACVP* basis set.^[21] Stationary point validation and thermodynamic contributions are obtained from gas phase vibrational calculations. The final energies (ΔG) are

composites obtained from adding the gas phase thermodynamic adjustment (including ZPE) to the final energies in solvent calculated with the continuum model at the converged gas phase geometries. All structures are inspected for interactions that may invalidate the use of gas phase geometries. We note that the approximations used here are usually valid for energy minima, but may be problematic for transition states if the reaction coordinate is coupled to a major electrostatic change.

Experimental Details

All reactions were performed under a nitrogen atmosphere using standard Schlenk techniques. The glassware was pre-dried at 150°C overnight before use. THF was distilled from sodium benzophenone ketyl. Dodecane, NMP, and phenyl triflate were distilled from calcium hydride under a nitrogen atmosphere. The kinetic study was performed in a Dewar flask and the temperature was held constant with a Lauda Compact Low-Temperature Thermostat RL 6 CP using ethanol as cooling liquid. Analysis was performed on a gas chromatograph with a flame ionization detector and a $30\text{ m} \times 0.25\text{ mm} \times 0.25\text{ mm}$ EQUITYTM-5 fused silica capillary column, with nitrogen as carrier gas. General temperature program: 70°C for 2 min, then up to 300°C at $18^\circ\text{C min}^{-1}$. Dodecane was used as an internal standard. NMR spectroscopic analysis was carried out on a Varian 400 MHz instrument using CDCl_3 as solvent, with shifts measured against TMS.

Low Temperature Reactivity

A 100-mL round-bottomed flask was charged with $\text{Fe}(\text{acac})_3$ (89 mg, 0.25 mmol), sealed with a rubber septum, then evacuated and refilled with nitrogen four times. The substrate (5 mmol), dodecane (1.14 mL, 5 mmol), NMP (1.1 mL) and THF (50 mL) were added at room temperature and the mixture was cooled to -20°C or -78°C . A solution of *n*-octylmagnesium bromide (3 mL, 2 M in diethyl ether, 6 mmol) was added dropwise *via* syringe to the reaction flask (-20°C), or in portions (0.3 mL every 20 min, -78°C), causing a color change from red-orange to dark brown. After 30 min or 200 min, respectively, a small amount (1 mL) of the mixture was quenched with saturated ammonium chloride (1 mL) or brine (1 mL, used for the N-heterocycles), filtered through a small silica plug, diluted with diethyl ether (1 mL) and analyzed by GC. The concentration of all components was determined using dodecane as an internal standard.

Initial-Rate Measurement

The kinetic investigation was carried out by varying the concentration of one component at a time and keeping the rest of the components constant at standard reaction conditions; THF (19.5 mL), dodecane (114 μL , 0.5 mmol), NMP (0.5 mL), phenyl triflate (81 μL , 0.5 mmol), *n*-octylmagnesium chloride (250 μL , 0.5 mmol, 2 M in THF) and $\text{Fe}(\text{acac})_3$ (250 μL , 0.025 mmol, 0.1 M in THF).

A round-bottomed flask fitted with a rubber septum and magnetic stirring bar was placed in Dewar flask at -25°C . To the round-bottomed flask was added THF, dodecane, NMP, phenyl triflate and *n*-octylmagnesium chloride. The

total THF volume was adjusted to 20 mL for each run. The reaction mixture was left to equilibrate for 20 min at the given temperature. A calibration sample was taken from the reaction mixture (100 μ L), quenched in ammonium chloride (aqueous) (1 mL), diluted in diethyl ether and analyzed by gas chromatography using dodecane as internal standard. The reaction was initiated by adding $\text{Fe}(\text{acac})_3$ (0.1 M in THF). Samples were withdrawn from the reaction mixture and treated as detailed above.

^1H NMR (400 MHz, CDCl_3) Spectroscopic Data

Methyl 4-octylbenzoate: δ = 0.86–0.89 (t, 3H), 1.25–1.31 (m, 10H), 1.58–1.61 (m, 2H), 2.63–2.67 (t, 2H), 3.90 (s, 3H), 7.23–7.25 (d, 2H), 7.93–7.96 ppm (d, 2H).

p-Trifluoromethyloctylbenzene: δ = 0.88 (t, 3H), 1.21–1.39 (m, 10H), 1.57–1.64 (m, 2H), 2.65 (t, 2H), 7.27 (d, 2H), 7.52 ppm (d, 2H).

2-Octylpyridine: δ = 0.88 ppm (t, 3H), 1.29 (m, 10H), 1.7 (m, 2H), 2.77 (t, 2H), 7.25 (m, 2H), 7.58 (t, 1H), 8.5 (d, 1H)

Acknowledgements

The current project is supported by the Swedish Research Council. The computations were performed on C3SE computing resources in Gothenburg. We are grateful to AstraZeneca for generous support and to Dr. Sten Nilsson Lill for helpful discussions regarding the calculations.

References

- a) J. S. Carey, D. Laffan, C. Thomson, M. T. Williams, *Org. Biomol. Chem.* **2006**, *4*, 2337–2347; b) R. W. Dugger, J. A. Ragan, D. H. B. Ripin, *Org. Process Res. Dev.* **2005**, *9*, 253–258; c) A. C. Frisch, M. Beller, *Angew. Chem.* **2005**, *117*, 680–695; *Angew. Chem. Int. Ed.* **2005**, *44*, 674–688; d) A. Zapf, M. Beller, *Top. Catal.* **2002**, *19*, 101–109.
- a) *Handbook of Organopalladium Chemistry for Organic Synthesis*, Vol. 1–2 (Ed.: E.-I. Negishi), Wiley-VCH, New York, **2002**; b) *Metal-Catalyzed Cross-Coupling Reactions*, Vol. 1, (Eds.: A. de Meijere, F. Diederich), Wiley-VCH, Weinheim, **2004**; c) *Transition Metals for Organic Synthesis*, Vol. 1, (Eds.: M. Beller, C. Bolm), Wiley-VCH, Weinheim, **2004**; d) J. Tsuji, *Palladium Reagents and Catalysts*, Vol. 1, Wiley, Chichester, **2004**.
- a) M. S. Kharasch, E. K. Fields, *J. Am. Chem. Soc.* **1941**, *63*, 2316–2320; b) M. S. Kharasch, P. O. Tawney, *J. Am. Chem. Soc.* **1941**, *63*, 2308–2315; c) M. S. Kharasch, M. Kleiman, *J. Am. Chem. Soc.* **1943**, *65*, 491–493.
- a) J. P. Corriu, J. P. Masse, *J. Chem. Soc. Chem. Commun.* **1972**, 144a–144a; b) K. Tamao, K. Sumitani, M. Kumada, *J. Am. Chem. Soc.* **1972**, *94*, 4374–4376.
- a) M. Tamura, J. Kochi, *J. Organomet. Chem.* **1971**, *31*, 289–309; b) M. Tamura, J. K. Kochi, *J. Am. Chem. Soc.* **1971**, *93*, 1487–1489; c) J. K. Kochi, *Acc. Chem. Res.* **1974**, *7*, 351–360; d) S. M. Neumann, J. K. Kochi, *J. Org. Chem.* **1975**, *40*, 599–606; e) G. A. Molander, B. J. Rahn, D. C. Shubert, S. E. Bonde, *Tetrahedron Lett.* **1983**, *24*, 5449–5452; f) J. K. Kochi, *J. Organomet. Chem.* **2002**, *653*, 11–19; g) T. Kauffmann, *Angew. Chem.* **1996**, *108*, 401–418; *Angew. Chem. Int. Ed. Engl.* **1996**, *35*, 386–403.
- a) R. B. Bedford, M. Betham, D. W. Bruce, A. A. Danopoulos, R. M. Frost, M. Hird, *J. Org. Chem.* **2006**, *71*, 1104–1110; b) R. B. Bedford, M. A. Hall, G. R. Hodges, M. Huwe, M. C. Wilkinson, *Chem. Commun.* **2009**, 6430–6432; c) R. B. Bedford, M. Huwe, M. C. Wilkinson, *Chem. Commun.* **2009**, 600–602; d) G. Cahiez, H. Avedissian, *Synthesis* **1998**, 1199–1205; e) G. Cahiez, V. Habiak, C. Duplais, A. Moyeux, *Angew. Chem.* **2007**, *119*, 4442–4444; *Angew. Chem. Int. Ed.* **2007**, *46*, 4364–4366; f) R. R. Chowdhury, A. K. Crane, C. Fowler, P. Kwong, C. M. Kozak, *Chem. Commun.* **2008**, 94–96; g) W. M. Czaplik, M. Mayer, A. Jacobi von Wangelin, *Angew. Chem.* **2009**, *121*, 616–620; *Angew. Chem. Int. Ed.* **2009**, *48*, 607–610; h) T. Nagano, T. Hayashi, *Org. Lett.* **2004**, *6*, 1297–1299; i) J. Norinder, A. Matsumoto, N. Yoshikai, E. Nakamura, *J. Am. Chem. Soc.* **2008**, *130*, 5858–5859; j) J. Quintin, X. Franck, R. Hocquemiller, B. Figadere, *Tetrahedron Lett.* **2002**, *43*, 3547–3549; k) I. Sapountzis, W. W. Lin, C. C. Kofink, C. Despotopoulou, P. Knochel, *Angew. Chem.* **2005**, *117*, 1682–1685; *Angew. Chem. Int. Ed.* **2005**, *44*, 1654–1657.
- S. Lou, G. C. Fu, *J. Am. Chem. Soc.* **2010**, *132*, 1264–1266.
- W. M. Czaplik, M. Mayer, J. Cvengros, A. Jacobi von Wangelin, *ChemSusChem* **2009**, *2*, 396–417.
- C. L. Kwan, J. K. Kochi, *J. Am. Chem. Soc.* **1976**, *98*, 4903–4912.
- R. S. Smith, J. K. Kochi, *J. Org. Chem.* **1976**, *41*, 502–509.
- a) A. Fuerstner, A. Leitner, M. Mendez, H. Krause, *J. Am. Chem. Soc.* **2002**, *124*, 13856–13863; b) A. Fuerstner, R. Martin, *Chem. Lett.* **2005**, *34*, 624–629.
- a) L. E. Aleandri, B. Bogdanovic, P. Bons, C. Duerr, A. Gaidies, T. Hartwig, S. C. Hockett, M. Lagarden, U. Wilczok, R. A. Brand, *Chem. Mater.* **1995**, *7*, 1153–1170; b) B. Bogdanovic, M. Schwickardi, *Angew. Chem.* **2000**, *112*, 4788–4790; *Angew. Chem. Int. Ed.* **2000**, *39*, 4610–4612; c) J. P. Collman, *Acc. Chem. Res.* **1975**, *8*, 342–347; d) A. Fuerstner, P. Hannen, *Chem. Eur. J.* **2006**, *12*, 3006–3019.
- a) J. Kleimark, A. Hedström, P.-F. Larsson, C. Johansson, P.-O. Norrby, *ChemCatChem* **2009**, *1*, 152–161.
- a) R. Martin, S. L. Buchwald, *J. Am. Chem. Soc.* **2007**, *129*, 3844–3845; b) A. Hedström, U. Bollmann, J. Bravidor, P.-O. Norrby, *Chem. Eur. J.* **2011**, *17*, 11991–11993.
- P. J. Alonso, A. B. Arauzo, J. Fornies, M. A. Garcia-Monforte, A. Martin, J. I. Martinez, B. Menjon, C. Rillo, J. J. Saiz-Garitaonandia, *Angew. Chem.* **2006**, *118*, 6859–6863; *Angew. Chem. Int. Ed.* **2006**, *45*, 6707–6711.
- C. L. McMullin, J. Jover, J. N. Harvey, N. Fey, *Dalton Trans.* **2010**, 39, 10833–10836.
- a) J. G. de Vries, P. H. Phua, L. Lefort, J. A. F. Boogers, M. Tristany, *Chem. Commun.* **2009**, 3747–3749; b) L. Lefort, C. Rangheard, C. D. Fernandez, P. H. Phua, J. Hoorn, J. G. de Vries, *Dalton Trans.* **2010**, 39, 8464–8471.
- Jaguar v. 7.6*, Schrödinger LLC, New York, NY, **2009**.

- [19] a) B. Marten, K. Kim, C. Cortis, R. A. Friesner, R. B. Murphy, M. N. Ringnalda, D. Sitkoff, B. Honig, *J. Phys. Chem.* **1996**, *100*, 11775–11788; b) D. J. Tannor, B. Marten, R. Murphy, R. A. Friesner, D. Sitkoff, A. Nicholls, M. Ringnalda, W. A. Goddard, B. Honig, *J. Am. Chem. Soc.* **1994**, *116*, 11875–11882.
- [20] a) A. D. Becke, *Phys. Rev. A* **1988**, *38*, 3098–3100; b) C. T. Lee, W. T. Yang, R. G. Parr, *Phys. Rev. B* **1988**, *37*, 785–789; c) P. J. Stephens, F. J. Devlin, C. F. Chabalowski, M. J. Frisch, *J. Phys. Chem.* **1994**, *98*, 11623–11627.
- [21] P. J. Hay, W. R. Wadt, *J. Chem. Phys.* **1985**, *82*, 299–310.
-